# The vertical distribution of iron stable isotopes in the North Atlantic near Bermuda

Seth G. John[1,2] and Jess Adkins[2]

Received 27 January 2011; revised 27 February 2012; accepted 2 May 2012; published 15 June 2012.

[1] Seawater dissolved iron isotope ratios ($\delta^{56}$Fe) have been measured in the North Atlantic near Bermuda. In a full-depth profile, seawater dissolved $\delta^{56}$Fe is isotopically heavy compared to crustal values throughout the water column ($\delta^{56}Fe_{IRMM\text{-}014}$ = +0.30‰ to +0.71‰). Iron isotope ratios are relatively homogenous in the upper water column (between +0.30‰ to +0.45‰ above 1500 m), and $\delta^{56}$Fe increases below this to a maximum of +0.71‰ at 2500 m, decreasing again to +0.35‰ at 4200 m. The $\delta^{56}$Fe profile is very different from the iron concentration profile; in the upper water column [Fe] is variable while $\delta^{56}$Fe is relatively constant, and in the deeper water column $\delta^{56}$Fe varies while [Fe] remains relatively constant. The $\delta^{56}$Fe profile is also not well correlated with other hydrographic tracers in the North Atlantic such as temperature, salinity, or the concentrations of oxygen, phosphate, silica, and CFC-11. The dissimilarity between $\delta^{56}$Fe profiles and profiles of [Fe] and other hydrographic tracers shows that Fe isotope ratios provide a unique sort of information about ocean chemistry, and they suggest that Fe isotopes may therefore be a valuable new tool for tracing the global sources, sinks, and biogeochemical cycling of Fe.

**Citation:** John, S. G., and J. Adkins (2012), The vertical distribution of iron stable isotopes in the North Atlantic near Bermuda, *Global Biogeochem. Cycles*, *26*, GB2034, doi:10.1029/2011GB004043.

## 1. Introduction

[2] Iron is a globally important micronutrient in the oceans, where the growth of phytoplankton is often limited by low iron concentrations. Controls on dissolved iron concentration in seawater are a key question in chemical oceanography, but the factors which control the distribution of iron in seawater are poorly understood. Significant sources of Fe to the oceans may include continental dust, hydrothermal vents, and continental-margin sediments. Within the oceans, Fe may be redistributed by biological processes such as Fe uptake and remineralization, and inorganic processes such as scavenging onto and release from sinking particulates. Measuring Fe concentrations in seawater provides valuable information about these processes, but new tracers, such as iron stable isotope ratios, provide an opportunity to further develop our understanding of the marine iron cycle.

[3] New techniques for extraction of Fe from seawater with low chemical blanks have made it possible to measure dissolved $\delta^{56}$Fe with sufficient accuracy to observe natural variation [*John and Adkins*, 2010; *Lacan et al.*, 2008, 2010; *Radic et al.*, 2011]. These variations have been attributed both to differences in the sources of iron to the ocean and to fractionation of Fe isotopes by chemical reaction in seawater. For example, in the Southern Ocean the isotopically light $\delta^{56}$Fe at 1250 m correlates with an oxygen minimum due to remineralization of organic material, and the heavier $\delta^{56}$Fe in surface waters could possibly be due to the biological fractionation of Fe isotopes [*Lacan et al.*, 2008]. Fe isotope signatures in the Equatorial Pacific are interpreted as tracing the non-reductive dissolution of sediments and water mass circulation [*Radic et al.*, 2011]. Dissolved $\delta^{56}$Fe in the San Pedro Basin ranges from −1.7‰ to 0.0‰ [*John et al.*, 2012], with the isotopically lightest iron found in the deepest waters suggesting a source of isotopically light iron from the reducing sediments [e.g., *Severmann et al.*, 2010; *Welch et al.*, 2003]. The heaviest iron isotope ratio in the San Pedro Basin is found in surface waters, suggesting atmospheric iron deposition into surface waters [*John et al.*, 2012].

[4] The use of $\delta^{56}$Fe as a tracer of the marine iron cycle is complicated, however, by the complex chemistry of iron in the oceans. Fe is a 'hybrid-type' element with profiles of Fe concentrations in seawater showing the behaviors both of a nutrient-type element and a scavenged element [*Bruland and Lohan*, 2003]. Fe concentrations typically decrease in surface waters where Fe is taken up as a nutrient, but Fe concentrations are lower in the Pacific than in the Atlantic, similar to a scavenged-type element [*Breitbarth et al.*, 2010, and references therein]. The relative importance of kinetic versus equilibrium controls on Fe concentrations in seawater

[1]Department of Earth and Ocean Sciences, University of South Carolina, Columbia, South Carolina, USA.
[2]Division of Geological and Planetary Sciences, California Institute of Technology, Pasadena, California, USA.

Corresponding author: S. G. John, Department of Earth and Ocean Sciences, University of South Carolina, Columbia, SC 29208, USA. (sjohn@geol.sc.edu)

are also a matter of debate. One perspective holds that Fe concentrations are primarily governed by an equilibrium where Fe solubility is held constant by a constant concentration of Fe-binding organic ligands in the deep ocean [e.g., *Johnson et al.*, 1997]. Another perspective is that a kinetic paradigm, with processes such as mineral dissolution, biological uptake, and biological remineralization, can explain the distribution of iron in the oceans [*Boyle*, 1997]. One way to differentiate between different models of iron cycling in the ocean is to compare the timescales of the reactions of Fe in the water column. The scavenging residence time for the deep Atlantic is estimated as 270 ± 140 years based on the decrease in NADW [Fe] along the flow path southwards [*Bergquist and Boyle*, 2006], whereas scavenging residence times in the deep North Pacific are 200 years calculated from Fe profiles [*Johnson et al.*, 1997] or 70 to 140 years based on dissolved/particulate Fe ratios [*Bruland et al.*, 1994]. In contrast, scavenging residence times in the surface ocean are typically shorter, for example modeling Fe distribution and scavenging at the BATS site in the North Atlantic yields scavenging residence times as low as 3 years at 100 m [*Weber et al.*, 2007]. Of course, long scavenging residence times do not mean that Fe is unreactive on shorter timescales. *Bacon and Anderson* [1982] posit a model for Th scavenging in the water column where Th atoms adsorb and desorb from particles many times as they sink to the ocean floor, such that the timescale for Th reaction is much faster than the net scavenging residence time. The same could be true of iron, though the factors which control the distribution of Fe in the oceans are not known. Fe isotopes may be a new tool to explore these processes.

[5] The sources of Fe to the oceans are also not fully constrained. Dust is known to be an important source of Fe to the open ocean [e.g., *Jickells et al.*, 2005; *Moore and Braucher*, 2008], with hydrothermal vents and reducing continental margin sediments also hypothesized as important contributors to the global marine iron pool. While Fe concentrations in pure hydrothermal fluid are typically quite high ($\mu$M to mM), most of that Fe precipitates in the immediate vicinity of the hydrothermal vents [*German et al.*, 1991]. Recent studies suggest that enough hydrothermal iron is stabilized during mixing with seawater to increase iron concentrations in the ocean [*Bennett et al.*, 2008; *Boyle and Jenkins*, 2008; *Tagliabue et al.*, 2010; *Toner et al.*, 2009]. However, previous studies differ on whether hydrothermal vents are a source of isotopically heavy or isotopically light Fe to the oceans compared to crustal values [*Bennett et al.*, 2009; *Severmann et al.*, 2004]. Reducing continental-margin sediments may also contribute to the global Fe pool, due to the high sedimentary fluxes of Fe(II) in these regions [*Elrod et al.*, 2004; *Moore et al.*, 2004], and this flux is associated with a characteristically light $\delta^{56}$Fe signature [*Severmann et al.*, 2010; *John et al.*, 2012] which suggests that seawater $\delta^{56}$Fe may be a valuable tracer for sources of Fe to the ocean. Oxidizing continental margin sediments may also be a source of Fe to the oceans, with a $\delta^{56}$Fe signature that appears to be slightly heavier than typical open-ocean dissolved $\delta^{56}$Fe [*Radic et al.*, 2011].

[6] Given the many questions that remain about the sources and sinks for Fe in the ocean, and the internal biogeochemical cycling of Fe within the ocean, Fe isotopes are a promising new tool to study the marine Fe cycle. However, little data is available on the distribution of iron isotopes in seawater or on the processes which control this distribution. Here, we present the first profile of dissolved $\delta^{56}$Fe from the North Atlantic ocean, and compare the distribution of iron isotopes to the distribution of other hydrographic tracers in the North Atlantic. Several preliminary hypotheses which could account for the observed distribution of Fe isotopes are explored as a way to constrain the possible factors which might control seawater $\delta^{56}$Fe.

## 2. Methods

[7] Seawater samples were collected as part of the first Geotraces Intercalibration cruise (R/V *Knorr*, June 22, 2008). Samples were collected at 31°40′N 64°10′W, the site of the Bermuda Atlantic Time series. Samples were collected using the U.S. Geotraces Clean Rosette which employs 12 L Teflon-coated GO-Flo bottles mounted on a polyurethane-coated frame suspended from a Kevlar hydrowire. Most samples were collected during a profile for trace element isotope intercalibration and acidified at sea in the sample bottles (GPrI). Samples from 2000 m were acidified in a large "deep sample" tank (GDI), and surface samples were collected using a trace-metal clean fish sampler and acidified in the large "surface sample" tank (GSI).

[8] Iron concentrations were measured by isotope dilution and precipitation. Ten mL subsamples of seawater were spiked with $^{57}$Fe and concentrated by a single coprecipitation with magnesium hydroxide after the addition of trace element clean ammonia (Seastar Chemicals,<10 ppt Fe) [*Wu and Boyle*, 1998]. Concentration samples were analyzed on a Neptune ICPMS with an SIS spray chamber inlet. All inlet components including nebulizer, spray chamber, torch, and cones were kept separate from those used for stable isotope analysis. Iron concentrations were also calculated based on the recovery of iron during our extraction and purification process, and these values are similar to those calculated by isotope dilution-ICPMS, typically within 0.1 nM. Seawater Fe concentrations calculated by isotope dilution are probably more accurate because they are insensitive to changes in extraction efficiency and/or variations in instrumental sensitivity. However, the agreement between these two different methods strengthens our confidence in the reproducibility and reliability of the NTA resin extraction procedure that we use for isotopic analysis.

[9] Iron for isotopic analysis was extracted from samples and analyzed for Fe isotope ratios using methods that have been optimized for analysis of seawater $\delta^{56}$Fe on 1 L samples [*John and Adkins*, 2010]. Briefly, Fe was concentrated by bulk extraction onto an NTA resin, rinsed with pH 2 water to remove excess salts, and further purified by anion exchange chromatography on AG-MP1 resin. Iron isotope ratios were measured on a Neptune multicollector ICP-MS using high-resolution mode to separate the $Fe^+$ ion beam from argide interferences. Both the accuracy and the precision of these measurements has been carefully documented based on extensive analysis of internal and external errors for 141 separate samples and process standards (Fe added to Fe-free seawater and extracted for purification analysis) [*John and Adkins*, 2010]. Accuracy in $\delta^{56}$Fe is 0.05‰ to

0.2‰ ($2\sigma$ external error) for 1 L seawater samples with 1 nM to 0.1 nM Fe, respectively.

## 3. Results

### 3.1. Fe and Fe Isotope Distribution

[10] Iron concentrations in the North Atlantic are typical of regions with high dust deposition (Figure 1 and Table 1). Iron concentrations are higher in the surface water (0.41 nM) and reach a minimum near the chlorophyll maximum (0.12 nM, 125 m). Below this depth, iron concentrations increase again to a maximum concentration (0.74 nM) at 2000 m. Our measurements of iron concentration in the SAFe intercalibration standards by isotope dilution (S: 0.10 ± 0.08 nM ($1\sigma$ SD $n$ = 4), D2: 0.89 ± 0.03 nM ($1\sigma$ SD $n$ = 4)) match well with the current consensus values (S: 0.094 ± 0.008 nM, D2: 0.923 ± 0.029 nM).

[11] Seawater dissolved $\delta^{56}$Fe in the North Atlantic is relatively homogeneous throughout the water column. For the ten depths, dissolved $\delta^{56}$Fe is between +0.30‰ and +0.45‰, except for samples from 2000 and 2500 m which are +0.55‰ and +0.71‰, respectively. This isotopic homogeneity is particularly surprising in light of the variability in iron concentration in the upper water column. In the deep ocean below 1500 m, the reverse is true and iron concentrations are more constant between 0.55 and 0.74 nM, while $\delta^{56}$Fe is more variable with an increase of almost 0.4‰ to a maximum at 2500 m.

### 3.2. Fe Isotope Distribution Compared to Other Hydrographic Tracers

[12] The influence of several different water masses can clearly be observed from a 1997 north-south section in the North Atlantic (Figure 2) and in hydrographic data collected concurrently with our sampling (Figure 1). The surface waters of the North Atlantic are warm and high in salinity. Below this, between 500 m to 1000 m at our sampling site, we see the influence of the oxygen-depleted Mediterranean Overflow Waters (MOW). From 1500 m to 4000 m is a broad region of North Atlantic Deep Water (NADW) which is formed by the sinking of surface waters at high latitudes. In the deepest North Atlantic, the influence of Antarctic Bottom Water (AABW) is seen primarily as a tongue of high-Si water intruding from the south.

[13] Fe concentrations at our study site display a nutrient-type profile, plus an atmospheric source of Fe to the ocean surface. Based on temperature, salinity, and fluorescence data, the mixed layer depth at the time of sampling was approximately 140 m and the chlorophyll maximum extended from roughly 120 to 140 m. Measured Fe concentrations were lowest at 75 m and 125 m, reflecting the biological uptake of Fe as a nutrient at these depths near the base of the mixed layer and the chlorophyll max. Increasing Fe concentrations over the thermocline between 125 m and 1000 m reflect the remineralization of sinking organic matter [*Bruland and Lohan*, 2003]. The deeper maximum in Fe concentrations, compared to phosphate, may reflect the slower remineralization of Fe or the influence of Fe scavenging by particles and subsequent release at depth. Fe concentrations are relatively homogeneous below 1000 m, similar to the homogeneity in other tracers within NADW. However, there is a marked decrease in Fe concentrations of about 0.15 nM between 2000 m and 2500 m. CFC-11 concentrations also decrease strongly across this interval, suggesting a possible relationship between [Fe] and water mass age or the region in which this water mass was formed. In the very surface waters, at 10 m, Fe concentrations are higher due to the deposition of iron-rich dust to the surface ocean.

[14] Iron isotopes, unlike the iron concentration profile, do not correlate well with most other hydrographic parameters (Figure 3). Fe isotope ratios do not change much in the upper 1500 m of the water column, despite large variations in every other tracer examined. Below this, the maximum in $\delta^{56}$Fe is seen at the core of NADW, but the distribution of NADW at our sample site is not well correlated to $\delta^{56}$Fe. NADW extends from 1500 m to 4000 m as classified by salinities of 34.9 to 35.0. Phosphate and oxygen show similarly broad and homogeneous distributions. There is a local minimum in oxygen concentrations near 3000 m, but the magnitude of this change (~5 $\mu$mol/kg) is very much smaller than variations in the thermocline (~100 $\mu$mol/kg) where $\delta^{56}$Fe does not vary. Si concentrations increase between 1500 m to 2500 m, as does $\delta^{56}$Fe, but this increase in Si is monotonic with even higher Si concentrations at greater depths while $\delta^{56}$Fe decreases at 4200 m. Similarly, concentrations of CFC-11 decrease monotonically between 1500 m and the ocean floor.

[15] The distribution of hydrothermal $\delta^3$(He) in the North Atlantic is somewhat similar to $\delta^{56}$Fe, in that both tracers have a sharp maximum in deep waters [*Jenkins and Clarke*, 1976]. Surface and mid-depth peaks in $\delta^3$(He) are attributed to the decay of tritium released during atmospheric testing of nuclear weapons, but the deep maximum observed throughout the western Atlantic Ocean is attributed to hydrothermal input, with the likely source of the deep hydrothermal $\delta^3$(He) peak near Bermuda being the Gibbs Fracture Zone at 50°N on the North Atlantic Ridge. The depth of the measured $\delta^3$(He) maximum near Bermuda is 3500 m compared to a maximum in $\delta^{56}$Fe measured at 2500 m, however the resolution of both profiles is sparse and there are no $\delta^{56}$Fe data between 2500 m and 4200 m. Insufficient vertical resolution hampers our ability to determine whether the true maximum of these tracers is the same or not.

[16] While there are not obvious correlations between $\delta^{56}$Fe and most other hydrographic tracers of NADW, it is possible that Fe isotope signals are tied to the specific location at which different components of NADW were formed. Generally, NADW is formed from North Atlantic surface water, which is high in salinity and sinks after cooling at northern latitudes. However, the homogeneity in many NADW tracers can mask more subtle differences within NADW, such that NADW can be divided into Upper North Atlantic Deep Water (UNADW), Northeast Atlantic Deep Water (NEADW), and Lower North Atlantic Deep Water (LNADW) [e.g., *Curry et al.*, 2003; *Talley*, 1996]. Following the NADW nomenclature of *Curry et al.* [2003] the heavier $\delta^{56}$Fe signals observed at 2000 m and 2500 m in our data correspond roughly to UNADW.

## 4. Discussion

[17] The dissimilarity between $\delta^{56}$Fe distribution in the North Atlantic and the distribution of other tracers

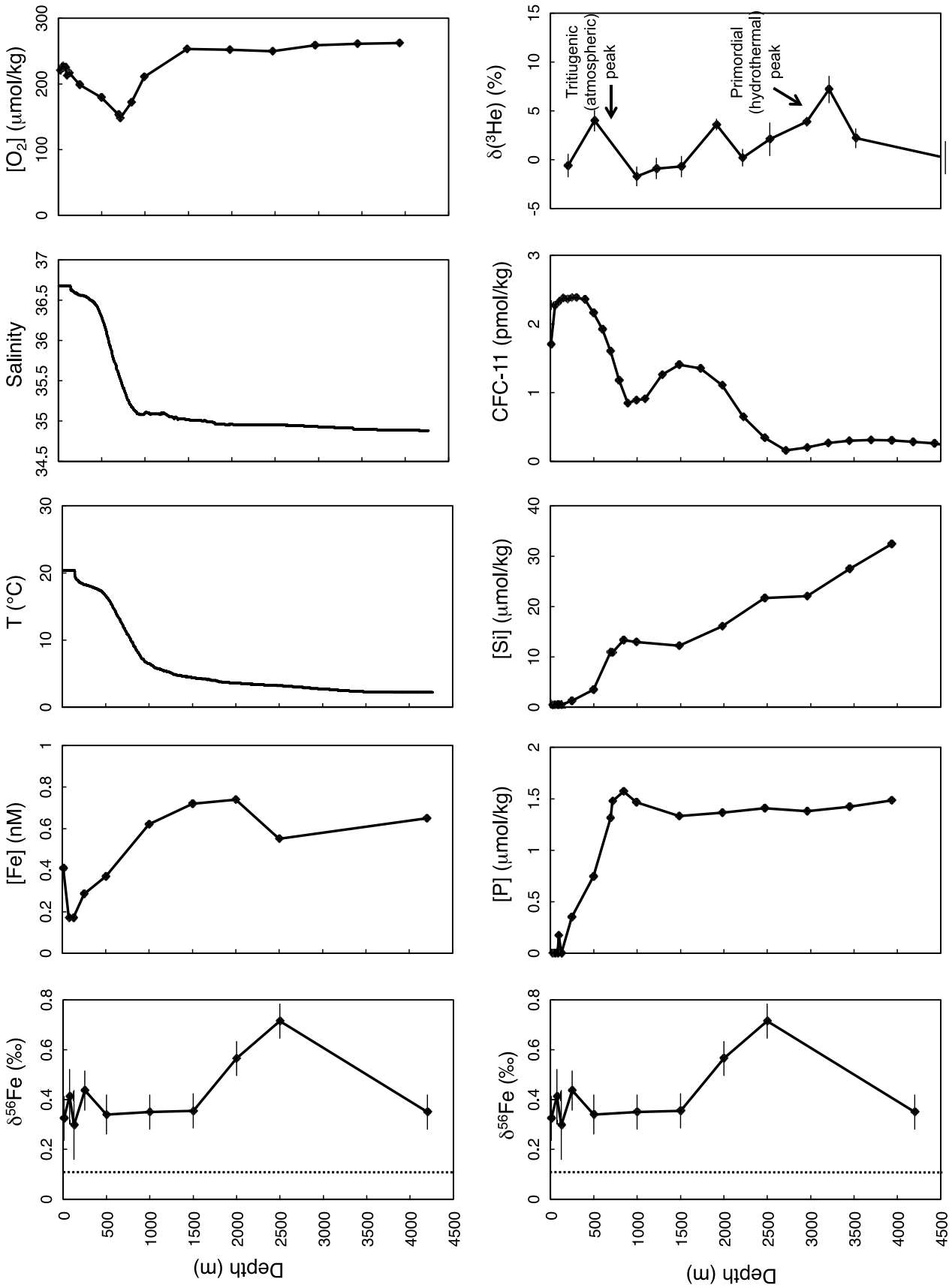
δ56Fe (‰)
[Fe] (nM)
T (°C)
Salinity
[O2] (μmol/kg)
δ(3He) (%)
Tritiugenic (atmospheric) peak
Primordial (hydrothermal) peak
CFC-11 (pmol/kg)
[Si] (μmol/kg)
[P] (μmol/kg)
Depth (m)

Figure 1

**Table 1.** Individual Sample Iron Isotope and Iron Concentration Data in the North Atlantic Near Bermuda (31°40′N 64°10′W, June 22, 2008)[a]

| Sample Name | GEOTRACES Sample Number | Depth (m) | T (°C) | Salinity | $\delta^{56}$Fe | Error ($2\sigma$)* | $\delta^{57/54}$Fe | [Fe] (nM) | n | Error ($1\sigma$ SD) |
|---|---|---|---|---|---|---|---|---|---|---|
| GSI-36 | GSI tank | 10 | 20.4 | 36.68 | 0.37 | 0.09 | 0.7 | 0.41 | 2 | 0.01 |
| GSI-36 | | 10 | | | 0.28 | 0.09 | 0.28 | | | |
| GPrI-43 | 2691 | 75 | 20.4 | 36.68 | 0.52 | 0.11 | 0.67 | 0.19 | 2 | 0.02 |
| GPrI-43 | | 75 | | | 0.30 | 0.11 | 0.5 | | | |
| GPrI-44 | 2691 | 75 | | | 0.48 | 0.11 | 0.88 | 0.15 | 2 | 0 |
| GPrI-44 | | 75 | | | 0.35 | 0.11 | 0.57 | | | |
| GPrI-35 | 2687 | 125 | 20.4 | 36.68 | 0.34 | 0.14 | 0.36 | 0.12 | 2 | 0.02 |
| GPrI-35 | | 125 | | | 0.14 | 0.14 | 0.32 | | | |
| GPrI-36 | 2687 | 125 | | | 0.36 | 0.14 | 0.69 | 0.19 | 2 | 0.01 |
| GPrI-37 | 2687/2688 | 125 | | | 0.36 | 0.14 | 0.7 | 0.2 | 2 | 0 |
| GPrI-37 | | 125 | | | 0.29 | 0.14 | 0.55 | | | |
| GPrI-28 | 2682 | 250 | 18.2 | 36.56 | 0.40 | 0.08 | 0.66 | 0.25 | 2 | 0.01 |
| GPrI-28 | | 250 | | | 0.41 | 0.08 | 0.59 | | | |
| GPrI-29 | 2682 | 250 | | | 0.50 | 0.08 | 0.88 | 0.32 | 2 | 0 |
| GPrI-22 | 2680 | 500 | 16.6 | 36.28 | 0.37 | 0.08 | 0.31 | 0.37 | 2 | 0.01 |
| GPrI-22 | | 500 | | | 0.31 | 0.08 | 0.45 | | | |
| GPrI-16 | 2677 | 1000 | 6.5 | 35.11 | 0.36 | 0.07 | 0.47 | 0.62 | 2 | 0.01 |
| GPrI-16 | | 1000 | | | 0.34 | 0.07 | 0.53 | | | |
| GPrI-11 | 2675 | 1500 | 4.4 | 35.01 | 0.35 | 0.07 | 0.52 | 0.72 | 2 | 0.02 |
| GPrI-11 | | 1500 | | | 0.36 | 0.07 | 0.54 | | | |
| GDI-35 | GDI tank | 2000 | 3.6 | 34.95 | | | | 0.74 | 2 | 0.01 |
| GDI-36 | | 2000 | | | 0.58 | 0.07 | 0.82 | | | |
| GDI-37 | | 2000 | | | 0.64 | 0.07 | 0.93 | | | |
| GDI-38 | | 2000 | | | 0.51 | 0.07 | 0.72 | | | |
| GDI-39 | | 2000 | | | 0.53 | 0.07 | 0.73 | | | |
| GPrI-8 | 2673/2674 | 2500 | 3.2 | 34.95 | 0.69 | 0.07 | 1.14 | 0.55 | 2 | 0.01 |
| GPrI-8 | | 2500 | | | 0.74 | 0.07 | 1.05 | | | |
| GT-4200 | | 4200 | 2.2 | 34.88 | 0.35 | 0.07 | 0.69 | 0.65 | 2 | 0.01 |
| SAFe S | | | | | | | | 0.1 | 4 | 0.08 |
| SAFe D2 | | | | | | | | 0.89 | 4 | 0.03 |

[a]All samples were collected on the GEOTRACES Intercalibration I cruise as part of the trace element isotopes intercalibration profile, and can be identified by their GEOTRACES sample names and numbers. Errors in $\delta^{56}$Fe for each sample are calculated according to *John and Adkins* [2010]. Iron concentrations by isotope dilution were measured on subsamples of the original sample carboys. Errors in iron concentration by isotope dilution are based on multiple analyses of the same subsample. Iron concentrations of SAFe intercalibration standards were measured by the same isotope dilution method, and our measured values match closely to consensus values.

demonstrates the potential value of $\delta^{56}$Fe. Because iron isotope distribution is mostly decoupled from the distribution of iron concentration and the distribution of other tracers, the information about marine biogeochemical cycles which is provided by $\delta^{56}$Fe is likely to be unique. In order to exploit this potentially valuable new tool, however, we must first understand the processes that control the distribution of Fe isotopes in seawater. Data from this single profile are not sufficient to conclusively determine the processes that lead to the observed $\delta^{56}$Fe profile in the North Atlantic. Nonetheless, we explore below some of the reactions of Fe in seawater and briefly discuss some hypotheses that may be consistent with our data. We hypothesize that the deep peak in $\delta^{56}$Fe might be due to either water mass properties associated with NEADW formation, or hydrothermal Fe input. We hypothesize that the isotopic homogeneity observed in the upper ocean might be due to either to a kinetic isotope effect during particulate Fe dissolution or to isotopic 'buffering' by isotopic equilibration between dissolved and particulate Fe pools.

### 4.1. Dissolved $\delta^{56}$Fe as a Tracer of Water Masses in the Deep Ocean

[18] While the deep maximum in $\delta^{56}$Fe in the North Atlantic is much sharper than the overall distribution of NADW, it is possible that Fe isotopes trace an aspect of the different components that comprise NADW. Specifically, the maximum in $\delta^{56}$Fe is roughly correlated with the occurrence of UNADW [*Curry et al.*, 2003; *Talley*, 1996]. It is possible that some aspect of the iron chemistry in surface waters in the UNADW outcrop region uniquely affects the iron isotope signature at 2000 to 2500 m at our site. Iron isotope signatures in the equatorial Pacific have been observed to persist over large horizontal distances, suggesting that they can be tied to specific water masses [*Radic et al.*, 2011], and the same might be true in the North Atlantic. We

**Figure 1.** Fe isotope and concentration data plotted alongside other hydrographic parameters from the North Atlantic near Bermuda. The dashed line plotted alongside $\delta^{56}$Fe represents the average iron isotope ratio of continental material [*Beard et al.*, 2003a). [Fe] data are taken from the same samples as $\delta^{56}$Fe. Temperature and salinity data are from the same cast as $\delta^{56}$Fe. Oxygen, phosphate, silica were sampled one day after [Fe]/$\delta^{56}$Fe was sampled. CFC-11 data are from the WOCE database for transect A22, station 54 (31.56°N 65.99°W). $\delta^{3}$He data was collected for the Geosecs-II intercalibration (35.8°N, 68.0°W) [*Jenkins et al.*, 1972]. Jenkins et al. attribute the surface peak in $\delta^{3}$He to the decay of bomb tritium, while the deepest peak is attributed to hydrothermal activity.

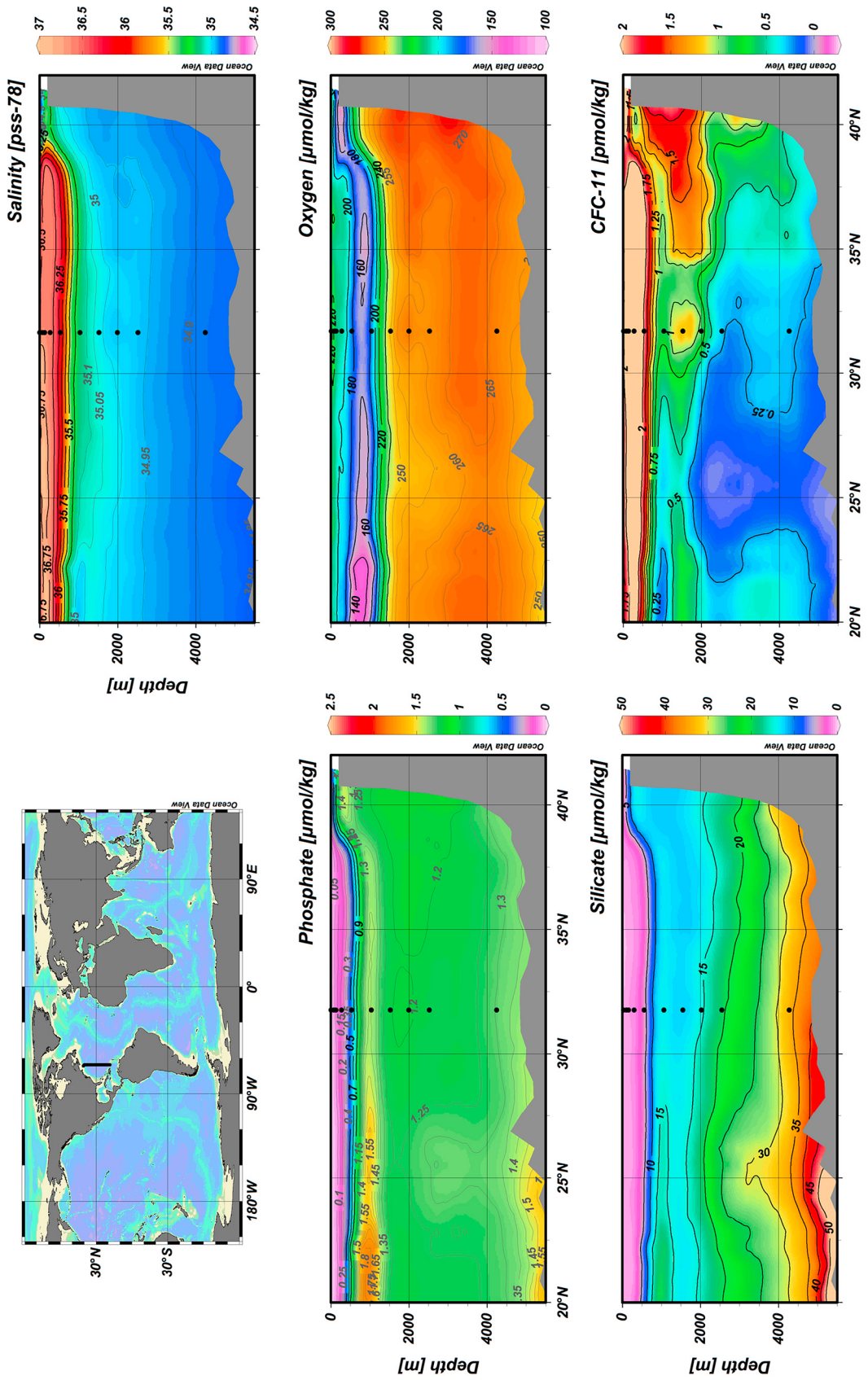


**Figure 2.** Hydrographic parameters in the North Atlantic along WOCE Section A22. The black points represent the approximate sampling location for our study. The influence of Antarctic Intermediate Water (AAIW) can be observed in low $O_2$ concentrations between ~500 m to ~1000 m. The influence of Antarctic Bottom Water (AABW) is observed most clearly in the high Si concentrations below ~5000 m. North Atlantic Deep Water (NADW), as defined by a salinity range from 34.9 to 35, extends roughly from 1500 m to 4000 m at our sampling location. The recent penetration of NADW into the deep ocean can be seen in the distribution of the modern anthropogenic tracer CFC-11. Plotted using Ocean Data View.

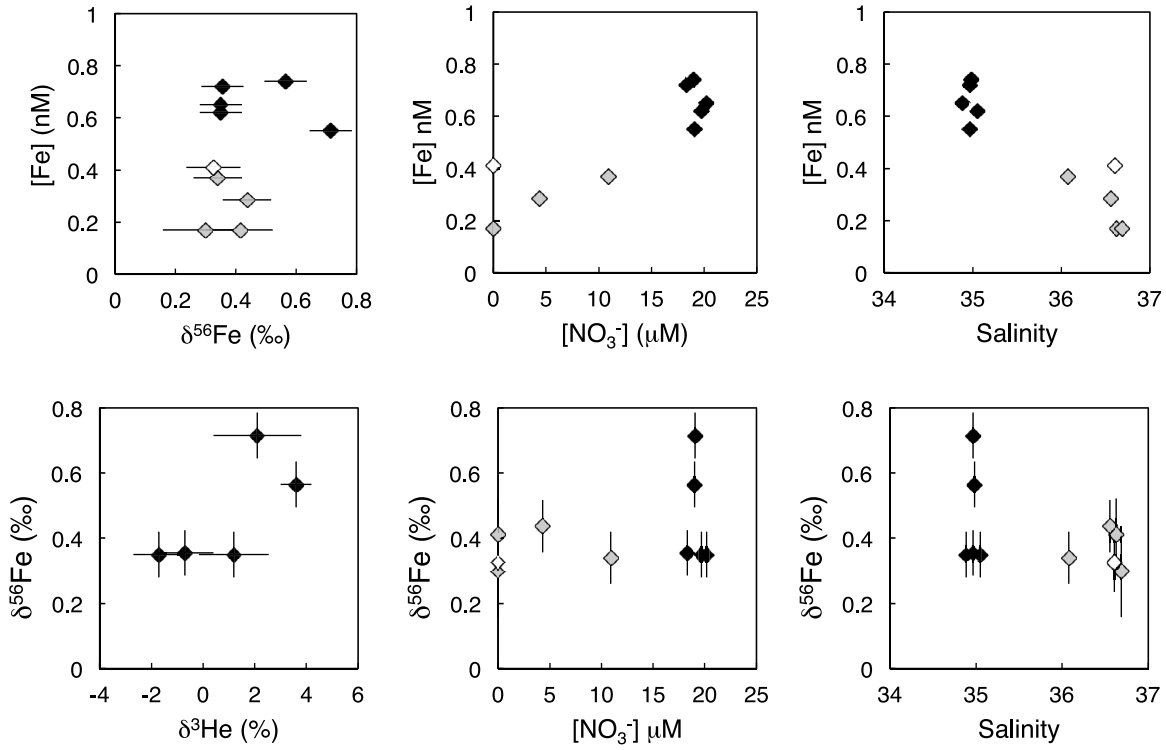


**Figure 3.** Cross plots of [Fe] and $\delta^{56}$Fe compared to other parameters at 5 m (white diamond) between 75 m to 500 m (gray diamonds), and between 1000 m to 4200 m (black diamonds). Nutrient and $\delta^{3}$He concentrations were interpolated from the closest sample based on potential temperature. Adjusted depths for most samples were within 20 m of the Fe/$\delta^{56}$Fe samples, except $\delta^{3}$He at 4200 m which was interpolated from values at 3500 m and 4500 m.

do not currently have a mechanistic explanation for the process which would cause NEADW to be isotopically heavy. There is no evidence of high $\delta^{56}$Fe values in our surface North Atlantic samples, so if some component of NADW is isotopically heavy at the point of formation, there must be an as yet unidentified process which enriches this water mass in heavier iron isotopes as it moves toward higher latitudes. While we can't rule out this water mass based explanation for the heavy $\delta^{56}$Fe peak at depth in our profile, we are motivated to search for other processes that might be at work.

### 4.2. Dissolved $\delta^{56}$Fe as a Tracer of Hydrothermal Fe Input to the Deep Ocean

[19] The vertical resolution of both $\delta^{56}$Fe and $\delta^{3}$He profiles near Bermuda is not sufficient to determine whether $\delta^{56}$Fe correlates with hydrothermal input. However, it is possible that hydrothermal Fe has a heavy iron isotope signature, and that hydrothermal dissolved Fe input is therefore responsible for the maximum in $\delta^{56}$Fe observed in our profile.

[20] Previous studies differ on whether hydrothermal vents are a source of isotopically heavy or isotopically light dissolved Fe to the oceans compared to crustal values. *Severmann et al.* [2004] found $\delta^{56}$Fe values in the Rainbow hydrothermal field were generally similar for primary hydrothermal fluids and sediments, and suspended particulates tended to be either similar to fluids or isotopically heavier than fluids. They concluded that Fe isotopes are conservative in hydrothermal plumes, implying a flux of isotopically light Fe to the oceans because most hydrothermal fluids are isotopically lighter than igneous rock by −0.2 to −0.3‰ [*Beard et al.*, 2003b; *Rouxel et al.*, 2004, 2008; *Severmann et al.*, 2004; *Sharma et al.*, 2001]. *Bennett et al.* [2009] found that hydrothermal particulates in a plume at 5°S on the Mid-Atlantic Ridge were isotopically lighter than the primary hydrothermal fluid, leading them to suggest that hydrothermal plumes would be a source of isotopically heavy dissolved Fe to the oceans. Both Fe(II)/Fe(III) equilibrium isotope effects and kinetic isotope effects during Fe precipitation are likely to be important in determining the $\delta^{56}$Fe of dissolved Fe in hydrothermal plumes. Fe(III)/Fe(II) redox chemistry typically fractionates Fe isotopes by 2 to 3 permil [*Balci et al.*, 2006; *Bullen et al.*, 2001; *Welch et al.*, 2003] with lighter isotopes preferentially concentrated in the seawater-soluble Fe(II) phase. Kinetic isotope effects of 0‰ to 2‰ have been observed during Fe precipitation, with preferential loss of lighter isotopes from the dissolved phase [*Balci et al.*, 2006; *Brantley et al.*, 2004; *Chapman et al.*, 2009; *Skulan et al.*, 2002]. Given the complex reactions of Fe in hydrothermal plumes, it seems possible that they could be a source of either isotopically heavy or isotopically light Fe to the oceans, depending on whether equilibrium or kinetic processes dominate. Both a better understanding of Fe isotope dynamics in hydrothermal plumes and more data on the marine distribution of $\delta^{56}$Fe are therefore necessary to determine whether the deep $\delta^{56}$Fe maximum observed at 2500 m near Bermuda is the result of hydrothermal input.

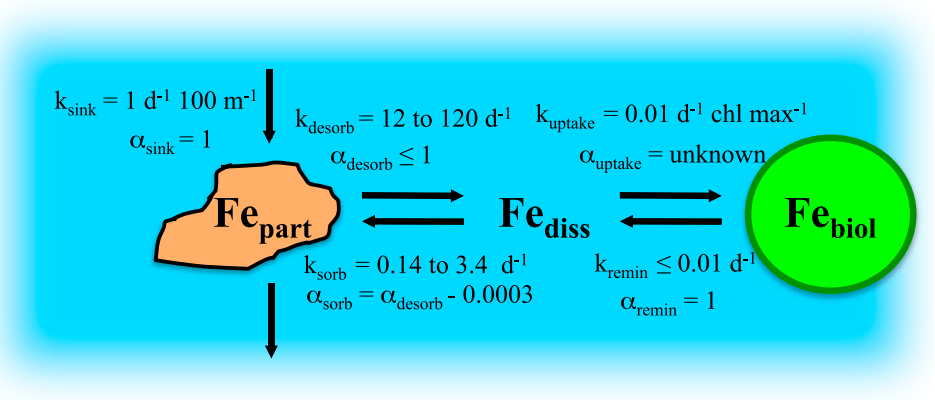


**Figure 4.** A simple model illustrates the estimated rate constants ($k$) and isotope effects ($\alpha$) for the reaction of iron in the ocean. The hypothetical 0.3 ‰ equilibrium isotope effect between dissolved and particulate Fe pictured here might be responsible for maintaining seawater $\delta^{56}$Fe between +0.3‰ to +0.45‰ in the upper North Atlantic, despite any biological Fe isotope fractionation.

### 4.3. Isotopic Fractionation During Fe Dissolution

[21] The simplest explanation for the observed isotopic homogeneity in the upper 1500 m in the North Atlantic is that $\delta^{56}$Fe input is +0.3‰ to +0.4‰, and there is no further fractionation of Fe isotopes. Dust is the primary source of iron to the surface North Atlantic [*Arimoto et al.*, 2003; *Jickells et al.*, 2005; *Moore and Braucher*, 2008], and the average isotopic composition of dust is similar to the crustal average of $\delta^{56}$Fe = +0.09 ‰ [*Beard et al.*, 2003a]. Control of surface seawater $\delta^{56}$Fe by isotopic fractionation during dust dissolution would therefore require an isotope effect of + 0.2‰ to +0.3‰, which preferentially releases heavier Fe isotopes from dust into seawater. By comparison, the dissolution of hornblende and goethite by strong organic ligands, and the dissolution of granite by oxalate-HCl, and the equilibrium fractionation between Fe(III) and hematite all preferentially release isotopically light or unchanged Fe [*Brantley et al.*, 2004; *Chapman et al.*, 2009; Skulan *et al.*, 2002]. However, a +0.2‰ isotope effect for dissolution of terrigenous sediments in seawater is inferred from seawater $\delta^{56}$Fe near Papua New Guinea, where deep waters interact with sediments on the continental shelves [*Radic et al.*, 2011].

[22] In order to maintain homogeneous $\delta^{56}$Fe over large changes in Fe concentration, there must also be minimal fractionation during biological uptake and remineralization. Based on increasing $\delta^{56}$Fe in surface ocean waters, the biological isotope effect for Fe uptake has been estimated as −0.25‰ to −0.13‰ in the Equatorial Pacific [*Radic et al.*, 2011], and −0.32‰ to +0.32 in the Southern Ocean. In the North Atlantic, we see no significant change in $\delta^{56}$Fe over the upper 1500 m of the water column, despite a 76% decrease in Fe concentration from 1500 m to 75 m. The current data does not allow us to distinguish whether the homogeneity in surface ocean $\delta^{56}$Fe reflects a lack of biological Fe isotope fractionation, or whether this fractionation is masked by other processes. The Fe isotope effect of biological remineralization is unknown.

### 4.4. Isotopic Buffering of $\delta^{56}$Fe in the Surface Ocean

[23] An alternative hypothesis to explain the isotopic homogeneity observed in the upper portion of our profile, despite biological fractionation of Fe isotopes, is the 'buffering' of dissolved $\delta^{56}$Fe by interaction with particles. In order to evaluate this hypothesis, we must calculate the rates at which different iron reactions take place in seawater. A simple reaction network for Fe in seawater would allow for exchange between inorganic particulate ($Fe_{particulate}$), dissolved ($Fe_{dissolved}$), and biological particulate ($Fe_{biological}$) phases with rate constants for iron transfer between phases being first order (Figure 4). The rate at which the particulate pool is renewed is determined by the flux of iron to the surface ocean and the sinking rate of particles. While colloids are known to be important intermediates in the transfer of Fe between particulate and soluble phases of Fe [*Honeyman and Santschi*, 1989, 1991; *Wen et al.*, 1997], a simplified model includes only particulate and dissolved (colloidal plus soluble) phases. The activity of colloids is therefore implied in the transfer of Fe between particulate and dissolved phases. Determining the rate constants for these various reactions is crucial for understanding iron isotopes, because the isotope ratio of Fe in seawater can be set by the reaction which equilibrates most quickly. The following is an assessment of how we estimate rate constants for these reactions.

[24] Biological iron uptake rates are calculated from organic carbon export rates in the Sargasso Sea and an Fe:N Redfield ratio. We use an organic carbon export of 3.4 mol $m^{-2}$ $yr^{-1}$ and an Fe:N biological uptake ratio of $\sim 3 \cdot 10^{-5}$ [*Weber et al.*, 2005] in order to calculate the rate of new biological Fe uptake. This corresponds to $2 \cdot 10^{-3}$ nM Fe $d^{-1}$ over a 20 m chlorophyll maximum. Assuming an iron concentration of 0.2 nM, the rate constant for net biological iron uptake ($k_{uptake}$) is 0.01 $d^{-1}$. The uptake of recycled biological iron is presumably much faster, but it is new production and export which are able to alter the total seawater $\delta^{56}$Fe. The remineralization rate constant in the thermocline ($k_{remin}$) is likely to be lower than $k_{uptake}$, assuming that remineralization takes place over a much longer length scale compared to biological productivity.

[25] We use several complementary techniques to estimate rates of iron exchange between the particulate and dissolved phases. $k_{desorb}$ can be estimated from the dissolution rates of

laboratory-produced amorphous ferric oxyhydroxides, which range from 20 $d^{-1}$ to 0.4 $d^{-1}$ for precipitates aged 1 min to 1 week [*Rose and Waite*, 2003]. Leaching of natural particulates are roughly consistent with these estimates. For example, iron dissolution has been measured for natural aerosols in seawater, where dissolution typically liberates a large pool of iron upon first contact with seawater (<5 min), followed by a slower release of iron over hours or days of continued leaching [*Aguilar-Islas et al.*, 2010; *Buck et al.*, 2006]. We assume that the first pulse of iron release into seawater is Fe(II) or very soluble iron salts, and so it is not representative of iron desorption rates from particles in the water column. By modeling first-order kinetics for the subsequent slower iron release, however, we can use particle leach data from seven aerosol samples from the Gulf of Alaska, equatorial Pacific, and subtropical Pacific [*Aguilar-Islas et al.*, 2010] to calculate a dissolution rate for the more slowly solubilizing iron pool ($k_{desorb}$) of 45 to 120 $d^{-1}$. These values are consistent with leaching of North Atlantic aerosols in natural seawater where 4% of particulate iron is soluble and 2% dissolves within the first hour, for a desorption rate constant ($k_{desorb}$) of 12 $d^{-1}$ [*Wu et al.*, 2007]. Also, the soluble fraction of Saharan dust was found to dissolve entirely in natural seawater within 1 day [*Mendez et al.*, 2010]. For the reverse reaction, we assume that release from organic ligands is the rate-limiting step for adsorption of dissolved iron on to particles and estimate that $k_{sorb}$ is therefore equal to $k_{unbinding}$ for seawater organic ligands. Values of $k_{unbinding}$ are 0.14 to 3.4 $d^{-1}$ in the North Atlantic above 1000 m [*Witter and Luther*, 1998].

[26] Our analysis of iron chemistry in seawater suggests that the rate constants for iron sorption and desorption from particles in the upper North Atlantic are greater than for biological uptake and remineralization, taking place on a timescale of hours to days compared to a timescale of days to longer for new biological uptake and remineralization (Figure 4). Exchange with particles is also much faster than estimates of iron's scavenging residence time, which range from 3 years in the surface North Atlantic to hundreds of years in the deep ocean [*Bergquist and Boyle*, 2006; *Bruland et al.*, 1994; *Johnson et al.*, 1997; *Weber et al.*, 2007]. This suggests that exchange with particles might buffer the $\delta^{56}$Fe of dissolved iron in seawater, provided that there is a large pool of particulate Fe available for exchange with the dissolved phase. In the North Atlantic, we predict that $k_{desorb}$ is greater than $k_{sorb}$, so the particulate Fe pool is actually much smaller than the dissolved pool. This is consistent with the findings of *Sherrell and Boyle* [1992] showing that total particulate Fe in the water column near Bermuda is generally between 0.1 to 1 nM, assuming that the exchangeable particulate Fe pool is a small fraction of the total. However, the particulate Fe pool is constantly renewed by the atmospheric deposition of dust and the sinking of this particulate material through the water column. With sinking rates of 10 to 100 m $d^{-1}$ [*Fowler and Knauer*, 1986], the particulate Fe pool will be renewed on a timescale of ~1 to 10 days over a 100 m mixed layer, or 10 to 100 days over the 1000 m thermocline, providing a constantly renewed source of iron for exchange with the dissolved phase. If an isotope buffer is responsible for maintaining homogeneous $\delta^{56}$Fe in the face of biological fractionation in the surface ocean, the flux of dust to the North Atlantic is therefore likely be crucial to this process.

## 5. Conclusions

[27] Seawater dissolved $\delta^{56}$Fe has been measured in the North Atlantic ocean near Bermuda. In the upper 1500 m in the North Atlantic, seawater dissolved $\delta^{56}$Fe is homogeneous within analytical error between +0.30 to +0.45 ‰. In the deeper ocean there is a peak in $\delta^{56}$Fe, with an apparent maximum of $\delta^{56}$Fe = +0.71‰ at 2500 m that is poorly constrained by low sampling resolution. We have explored the hypotheses that deep ocean $\delta^{56}$Fe in the North Atlantic is a tracer for water masses or is controlled by hydrothermal venting, and the hypotheses that upper ocean $\delta^{56}$Fe is controlled by a one-way isotope effect during particle dissolution or by isotopic buffering by particulates. Further data will be necessary to fully evaluate these hypotheses. The distribution of $\delta^{56}$Fe in the North Atlantic near Bermuda is very different than the Fe concentration profile, and it is different from most other tracers of water column chemistry. This suggests that $\delta^{56}$Fe provides valuable data about the marine biogeochemical cycling of Fe that cannot be obtained from studying other tracers. However, a greater understanding of the processes that control the distribution of Fe isotopes in the ocean is needed for this new tool to be most effectively used.

[28] **Acknowledgments.** Thanks to all who helped and participated on the Geotraces Intercalibration I cruise, especially Chief Scientist Greg Cutter, Ed Boyle, Geoffrey Smith, and the captain and crew of the R/V *Knorr*.

## References

Aguilar-Islas, A. M., J. Wu, R. Rember, A. M. Johansen, and L. M. Shank (2010), Dissolution of aerosol-derived iron in seawater: Leach solution chemistry, aerosol type, and colloidal iron fraction, *Mar. Chem.*, *120*, 25–33, doi:10.1016/j.marchem.2009.01.011.

Arimoto, R., R. A. Duce, B. J. Ray, and U. Tomza (2003), Dry deposition of trace elements to the western North Atlantic, *Global Biogeochem. Cycles*, *17*(1), 1010, doi:10.1029/2001GB001406.

Bacon, M. P., and R. F. Anderson (1982), Distribution of thorium isotopes between dissolved and particulate forms in the deep sea, *J. Geophys. Res.*, *87*, 2045–2056, doi:10.1029/JC087iC03p02045.

Balci, N., T. D. Bullen, K. Witte-Lien, W. C. Shanks, M. Motelica, and K. W. Mandernack (2006), Iron isotope fractionation during microbially stimulated Fe(II) oxidation and Fe(III) precipitation, *Geochim. Cosmochim. Acta*, *70*, 622–639, doi:10.1016/j.gca.2005.09.025.

Beard, B. L., C. M. Johnson, J. L. Skulan, K. H. Nealson, L. Cox, and H. Sun (2003a), Application of Fe isotopes to tracing the geochemical and biological cycling of Fe, *Chem. Geol.*, *195*, 87–117, doi:10.1016/S0009-2541(02)00390-X.

Beard, B. L., C. M. Johnson, K. L. Von Damm, and R. L. Poulson (2003b), Iron isotope constraints on Fe cycling and mass balance in oxygenated Earth oceans, *Geology*, *31*, 629–632, doi:10.1130/0091-7613(2003)031<0629:IICOFC>2.0.CO;2.

Bennett, S. A., E. P. Achterberg, D. P. Connelly, P. J. Statharn, G. R. Fones, and C. R. Gernian (2008), The distribution and stabilisation of dissolved Fe in deep-sea hydrothermal plumes, *Earth Planet. Sci. Lett.*, *270*, 157–167, doi:10.1016/j.epsl.2008.01.048.

Bennett, S. A., O. Rouxel, K. Schmidt, D. Garbe-Schonberg, P. J. Statham, and C. R. German (2009), Iron isotope fractionation in a buoyant hydrothermal plume, 5°S Mid-Atlantic Ridge, *Geochim. Cosmochim. Acta*, *73*, 5619–5634, doi:10.1016/j.gca.2009.06.027.

Bergquist, B. A., and E. A. Boyle (2006), Dissolved iron in the tropical and subtropical Atlantic Ocean, *Global Biogeochem. Cycles*, *20*, GB1015, doi:10.1029/2005GB002505.

Boyle, E. (1997), What controls dissolved iron concentrations in the world ocean? A comment, *Mar. Chem.*, *57*, 163–167, doi:10.1016/S0304-4203(97)00044-3.

Boyle, E., and W. Jenkins (2008), Hydrothermal iron in the deep western South Pacific, *Geochim. Cosmochim. Acta*, *72*, A107–A107.

Brantley, S. L., L. J. Liermann, R. L. Guynn, A. Anbar, G. A. Icopini, and J. Barling (2004), Fe isotopic fractionation during mineral dissolution with and without bacteria, *Geochim. Cosmochim. Acta*, *68*, 3189–3204, doi:10.1016/j.gca.2004.01.023.

Breitbarth, E., et al. (2010), Iron biogeochemistry across marine systems—Progress from the past decade, *Biogeosciences*, *7*, 1075–1097, doi:10.5194/bg-7-1075-2010.

Bruland, K. W., and M. C. Lohan (2003), *Controls of Trace Metals in Seawater*, Elsevier, Amsterdam.

Bruland, K. W., K. J. Orians, and J. P. Cowen (1994), Reactive trace-metals in the stratified central North Pacific, *Geochim. Cosmochim. Acta*, *58*, 3171–3182, doi:10.1016/0016-7037(94)90044-2.

Buck, C. S., W. M. Landing, J. A. Resing, and G. T. Lebon (2006), Aerosol iron and aluminum solubility in the northwest Pacific Ocean: Results from the 2002 IOC cruise, *Geochem. Geophys. Geosyst.*, *7*, Q04M07, doi:10.1029/2005GC000977.

Bullen, T. D., A. F. White, C. W. Childs, D. V. Vivit, and M. S. Schulz (2001), Demonstration of significant abiotic iron isotope fractionation in nature, *Geology*, *29*, 699–702, doi:10.1130/0091-7613(2001)029<0699:DOSAII>2.0.CO;2.

Chapman, J. B., D. J. Weiss, Y. Shan, and M. Lemburger (2009), Iron isotope fractionation during leaching of granite and basalt by hydrochloric and oxalic acids, *Geochim. Cosmochim. Acta*, *73*, 1312–1324, doi:10.1016/j.gca.2008.11.037.

Curry, R., B. Dickson, and I. Yashayaev (2003), A change in the freshwater balance of the Atlantic Ocean over the past four decades, *Nature*, *426*, 826–829, doi:10.1038/nature02206.

Elrod, V. A., W. M. Berelson, K. H. Coale, and K. S. Johnson (2004), The flux of iron from continental shelf sediments: A missing source for global budgets, *Geophys. Res. Lett.*, *31*, L12307, doi:10.1029/2004GL020216.

Fowler, S. W., and G. A. Knauer (1986), Role of large particles in the transport of elements and organic compounds through the oceanic water column, *Prog. Oceanogr.*, *16*, 147–194, doi:10.1016/0079-6611(86)90032-7.

German, C. R., A. C. Campbell, and J. M. Edmond (1991), Hydrothermal scavenging at the Mid-Atlantic Ridge: Modification of trace-element dissolved fluxes, *Earth Planet. Sci. Lett.*, *107*, 101–114, doi:10.1016/0012-821X(91)90047-L.

Honeyman, B. D., and P. H. Santschi (1989), A Brownian-pumping model for oceanic trace-metal scavenging: Evidence from Th isotopes, *J. Mar. Res.*, *47*, 951–992, doi:10.1357/002224089785076091.

Honeyman, B. D., and P. H. Santschi (1991), Coupling adsorption and particle aggregation: Laboratory studies of colloidal pumping using $^{59}$Fe-labeled hematite, *Environ. Sci. Technol.*, *25*, 1739–1747, doi:10.1021/es00022a010.

Jenkins, W. J., and W. B. Clarke (1976), Distribution of $^{3}$He in the western Atlantic Ocean, *Deep Sea Res.*, *23*, 481–494.

Jenkins, W. J., M. A. Beg, W. B. Clarke, P. J. Wangersky, and H. Craig (1972), Excess $^{3}$He in the Atlantic Ocean, *Earth Planet. Sci. Lett.*, *16*, 122, doi:10.1016/0012-821X(72)90245-2.

Jickells, T. D., et al. (2005), Global iron connections between desert dust, ocean biogeochemistry, and climate, *Science*, *308*, 67–71, doi:10.1126/science.1105959.

John, S. G., and J. F. Adkins (2010), Analysis of dissolved iron isotopes in seawater, *Mar. Chem.*, *119*, 65–76, doi:10.1016/j.marchem.2010.01.001.

John, S. G., J. Moffett, J. Mendez, and J. Adkins (2012), The flux of iron and iron isotopes from reducing sediments in the San Pedro Basin, *Geochim. Cosmochim. Acta*, in press.

Johnson, K. S., R. M. Gordon, and K. H. Coale (1997), What controls dissolved iron concentrations in the world ocean?, *Mar. Chem.*, *57*, 137–161, doi:10.1016/S0304-4203(97)00043-1.

Lacan, F., A. Radic, C. Jeandel, F. Poitrasson, G. Sarthou, C. Pradoux, and R. Freydier (2008), Measurement of the isotopic composition of dissolved iron in the open ocean, *Geophys. Res. Lett.*, *35*, L24610, doi:10.1029/2008GL035841.

Lacan, F., A. Radic, M. Labatut, C. Jeandel, F. Poitrasson, G. Sarthou, C. Pradoux, J. Chmeleff, and R. Freydier (2010), High-precision determination of the isotopic composition of dissolved iron in iron depleted seawater by double spike multicollector-ICPMS, *Anal. Chem.*, *82*, 7103–7111, doi:10.1021/ac1002504.

Mendez, J., C. Guieu, and J. Adkins (2010), Atmospheric input of manganese and iron to the ocean: Seawater dissolution experiments with Saharan and North American dusts, *Mar. Chem.*, *120*, 34–43, doi:10.1016/j.marchem.2008.08.006.

Moore, J. K., and O. Braucher (2008), Sedimentary and mineral dust sources of dissolved iron to the world ocean, *Biogeosciences*, *5*, 631–656, doi:10.5194/bg-5-631-2008.

Moore, J. K., S. C. Doney, and K. Lindsay (2004), Upper ocean ecosystem dynamics and iron cycling in a global three-dimensional model, *Global Biogeochem. Cycles*, *18*, GB4028, doi:10.1029/2004GB002220.

Radic, A., F. Lacan, and J. W. Murray (2011), Iron isotopes in the seawater of the equatorial Pacific Ocean: New constraints for the oceanic iron cycle, *Earth Planet. Sci. Lett.*, *306*, 1–10, doi:10.1016/j.epsl.2011.03.015.

Rose, A. L., and T. D. Waite (2003), Kinetics of hydrolysis and precipitation of ferric iron in seawater, *Environ. Sci. Technol.*, *37*, 3897–3903, doi:10.1021/es034102b.

Rouxel, O., Y. Fouquet, and J. N. Ludden (2004), Subsurface processes at the Lucky Strike hydrothermal field, Mid-Atlantic Ridge: Evidence from sulfur, selenium, and iron isotopes, *Geochim. Cosmochim. Acta*, *68*, 2295–2311, doi:10.1016/j.gca.2003.11.029.

Rouxel, O., W. C. Shanks, W. Bach, and K. J. Edwards (2008), Integrated Fe- and S-isotope study of seafloor hydrothermal vents at East Pacific Rise 9–10°N, *Chem. Geol.*, *252*, 214–227, doi:10.1016/j.chemgeo.2008.03.009.

Severmann, S., C. M. Johnson, B. L. Beard, C. R. German, H. N. Edmonds, H. Chiba, and D. R. H. Green (2004), The effect of plume processes on the Fe isotope composition of hydrothermally derived Fe in the deep ocean as inferred from the Rainbow vent site, Mid-Atlantic Ridge, 36°14′N, *Earth Planet. Sci. Lett.*, *225*, 63–76, doi:10.1016/j.epsl.2004.06.001.

Severmann, S., J. McManus, W. M. Berelson, and D. E. Hammond (2010), The continental shelf benthic iron flux and its isotope composition, *Geochim. Cosmochim. Acta*, *74*, 3984–4004, doi:10.1016/j.gca.2010.04.022.

Sharma, M., M. Polizzotto, and A. D. Anbar (2001), Iron isotopes in hot springs along the Juan de Fuca Ridge, *Earth Planet. Sci. Lett.*, *194*, 39–51, doi:10.1016/S0012-821X(01)00538-6.

Sherrell, R. M., and E. A. Boyle (1992), The trace-metal composition of suspended particles in the oceanic water column near Bermuda, *Earth Planet. Sci. Lett.*, *111*, 155–174, doi:10.1016/0012-821X(92)90176-V.

Skulan, J. L., B. L. Beard, and C. M. Johnson (2002), Kinetic and equilibrium Fe isotope fractionation between aqueous Fe(III) and hematite, *Geochim. Cosmochim. Acta*, *66*, 2995–3015, doi:10.1016/S0016-7037(02)00902-X.

Tagliabue, A., et al. (2010), Hydrothermal contribution to the oceanic dissolved iron inventory, *Nat. Geosci.*, *3*, 252–256, doi:10.1038/ngeo818.

Talley, L. D. (1996), North Atlantic circulation and variability, reviewed for the CNLS conference, *Physica D*, *98*, 625–646, doi:10.1016/0167-2789(96)00123-6.

Toner, B. M., S. C. Fakra, S. J. Manganini, C. M. Santelli, M. A. Marcus, J. Moffett, O. Rouxel, C. R. German, and K. J. Edwards (2009), Preservation of iron(II) by carbon-rich matrices in a hydrothermal plume, *Nat. Geosci.*, *2*, 197–201, doi:10.1038/ngeo433.

Weber, L., C. Volker, M. Schartau, and D. A. Wolf-Gladrow (2005), Modeling the speciation and biogeochemistry of iron at the Bermuda Atlantic Time-series Study site, *Global Biogeochem. Cycles*, *19*, GB1019, doi:10.1029/2004GB002340.

Weber, L., C. Volker, A. Oschlies, and H. Burchard (2007), Iron profiles and speciation of the upper water column at the Bermuda Atlantic Time-series Study site: A model based sensitivity study, *Biogeosciences*, *4*, 689–706, doi:10.5194/bg-4-689-2007.

Welch, S. A., B. L. Beard, C. M. Johnson, and P. S. Braterman (2003), Kinetic and equilibrium Fe isotope fractionation between aqueous Fe(II) and Fe(III), *Geochim. Cosmochim. Acta*, *67*, 4231–4250, doi:10.1016/S0016-7037(03)00266-7.

Wen, L. S., P. H. Santschi, and D. G. Tang (1997), Interactions between radioactively labeled colloids and natural particles: Evidence for colloidal pumping, *Geochim. Cosmochim. Acta*, *61*, 2867–2878, doi:10.1016/S0016-7037(97)00139-7.

Witter, A. E., and G. W. Luther (1998), Variation in Fe-organic complexation with depth in the northwestern Atlantic Ocean as determined using a kinetic approach, *Mar. Chem.*, *62*, 241–258, doi:10.1016/S0304-4203(98)00044-9.

Wu, J. F., and E. A. Boyle (1998), Determination of iron in seawater by high-resolution isotope dilution inductively coupled plasma mass spectrometry after $Mg(OH)_2$ coprecipitation, *Anal. Chim. Acta*, *367*, 183–191, doi:10.1016/S0003-2670(98)00145-7.

Wu, J., R. Rember, and C. Cahill (2007), Dissolution of aerosol iron in the surface waters of the North Pacific and North Atlantic Oceans as determined by a semicontinuous flow-through reactor method, *Global Biogeochem. Cycles*, *21*, GB4010, doi:10.1029/2006GB002851.